Transient Thermal Behavior of a Thermally and Elastically Orthotropic Medium

Hongsheng Wang* and Tsu-Wei Chou†
University of Delaware, Newark, Delaware

Transient two-dimensional temperature and stress distributions are examined for a thermally and elastically orthotropic slab with a rectangular boundary. The slab, initially held at a uniform temperature, is suddenly subjected to an arbitrary variation of temperature, heat flow, or convection on one edge (or surface) of the rectangle, while each of the remaining edges is either insulated or maintained at the initial temperature. A general solution has been obtained for the two-dimensional transient temperature distribution in the slab by use of the principle of superposition. Specific solutions corresponding to eight sets of boundary conditions are tabulated. As an application of the transient temperature solutions, the thermal stress distributions are investigated for one set of the boundary value problems. Numerical results for a typical unidirectional fiber-reinforced composite have demonstrated high concentrations of thermal stresses far exceeding those generated in a steady-state thermal environment.

Nomenclature

$A_{k,j}(\nu_k)$, $A_{km,j}(\nu_k,\mu_m)$	= coefficients in series expansion for T
A_{ij}	= elastic stiffness coefficients
a_j, b_j	= parameters defining thermal boundary conditions in Eqs. (3a-d)
B_k, B_{km}	= coefficients in series expansion of Eqs. (34) and (35)
C_{ij}	= coefficients in series expansion of Eq. (36) for Φ_j
D	= thermal diffusivity
E_{jk}	= material constants, defined in Eq. (44)
$f(y)$	= variation of surface condition along edge $z=\ell_2$
K	$=\sqrt{K_z/K_y}$
K_z, K_y	= coefficients of heat conduction in y and z directions, respectively
ℓ_1, ℓ_2	= lengths of the slab in y and z directions, respectively
t	= time
T	= temperature
v, w	= deflections in y and z directions, respectively
x,y,z	= rectangular Cartesian coordinates
β_1,β_2,β_3	= stress-temperature coefficients
γ_k	= material constant, defined in Eq. (41)
μ,γ	= constants introduced in Eqs. (37), (39), and (42)
ν_k,μ_m	= eigenvalues
ρ	= material constant, defined in Eq. (42)
$\sigma_{xx},\sigma_{yy},\sigma_{zz},\sigma_{yz}$	= stress components
ϕ,ψ	= temperature components, defined in Eq. (4)
ψ_j,Φ_j	= displacement potentials

I. Introduction

THE thermomechanical behavior of anisotropic elastic media has attracted considerable research interest in recent years due to the increasing engineering applications of these media in situations involving severe thermal environments. Fiber-reinforced composites are certainly well-known examples of both thermal and elastic anisotropy. The thermal response of composites is an important consideration not only in their fabrication and processing but also for material durability and long-term performance. These concerns have generated the need to find theoretical and experimental solutions to various problems involving anisotropic media. However, owing to the mathematical complexity in dealing with both the heat transfer and thermoelastic problems, exact theoretical solutions have been obtained for only very limited classes of problems. Experimental work in this area is also very scarce.

Recent investigations of anisotropic heat conduction have produced solutions based on a variety of methods, including transformation theory,[1-2] Green's function,[2-4] complex variable theory,[5] and finite difference.[6] The solution of the steady-state thermoelastic problem of anisotropic material appears to be initiated by Sharma,[7] Mussakowska and Nowacki,[8] and Singh.[9] Then, Sugano,[10] Sugano and Takeuti,[11] Takeuti and Noda,[12] and Noda[13] solved the transient temperature and thermal stress fields of transversely isotropic body for the case of prescribed surface temperature.

In the category of thermally and elastically orthotropic media, Tauchert and Aköz were first to investigate the steady-state temperature and thermal stress fields. They solved the problems involving a semi-infinite domain,[14] a slab bounded by two parallel infinite planes,[15] and a rectangular slab[16] with prescribed surface temperature. More recently, Wang and Chou[17] reported the transient thermal stress analysis using the displacement-potential approach for an orthotropic slab with a specific case of boundary conditions.

The present work reports the general solution method for analyzing the transient thermal behavior of a rectangular slab that is both thermally and elastically orthotropic. First, the general solution of the transient two-dimensional heat-conduction problem with a nonhomogeneous boundary condition (i.e., the slab is subjected to arbitrary heating on one surface) has been obtained by using the principle of superposition. Then, for the convenience of readers interested in the practical applications of the analysis, the specific solutions corresponding to eight sets of boundary conditions are

Received Nov. 23, 1984.

*Visiting Scholar, Department of Mechanical and Aerospace Engineering, Center for Composite Materials; presently at Research and Development Division, Chengdu Aircraft Company, China.

†Professor, Department of Mechanical and Aerospace Engineering, Center for Composite Materials.

tabulated. Second, as an application of the thermal boundary value problem solution, the induced thermal stress distribution in the orthotropic slab is presented. Numerical examples for the case simulating a unidirectional fiber-reinforced composite material are worked out for demonstrating the influences of thermal and elastic anisotropy.

The research on the thermal response of orthotropic materials should have particularly significant implications in the understanding of the thermomechanical behavior of fiber composites. An array of problems involving, for instance, boundary layers and interfaces under severe thermal condition all deserve in-depth assessment and examination in the future.

II. Transient Temperature Field

Consider the two-dimensional problem of an orthotropic body with a rectangular region $0<y<\ell_1$, $0<z<\ell_2$ (Fig. 1). Assume that the slab is initially held at a uniform temperature U_∞ like the surrounding medium and that one edge (surface) of the rectangle ($z=\ell_2$) is suddenly subjected to an arbitrary distribution of temperature or heat flux $f(y)$. The purpose of the study is to find the transient temperature distribution of the slab first.

The two-dimensional temperature distribution, $T(y,z;t) = U(y,z;t) - U_\infty$, in the rectangular region is assumed to satisfy the transient heat conduction equation

$$\frac{\partial^2 T}{\partial y^2} + K^2 \frac{\partial^2 T}{\partial z^2} = \frac{1}{D}\frac{\partial T}{\partial t} \tag{1}$$

Here $K^2 = K_z/K_y$ is the ratio of the conductivities in the z and y directions, respectively; $D = K_y/c\rho$ is the thermal diffusivity (by Kelvin) in the y direction; c, ρ are, respectively, the mass density and specific heat of the slab material; D, K_y, and K_z are assumed to be independent of temperature; t denotes time.

The initial condition assumes the following form

$$T(y,z;0) = U(y,z;0) - U_\infty = 0 \quad \text{for } t=0 \tag{2}$$

and the thermal boundary (or surface) conditions on the edges of the rectangle are expressed here in the general form of linear heat transfer

$$-a_1 \frac{\partial T}{\partial y} + b_1 T = 0 \qquad \text{for } y=0 \tag{3a}$$

$$a_2 \frac{\partial T}{\partial y} + b_2 T = 0 \qquad y=\ell_1 \tag{3b}$$

$$-a_3 \frac{\partial T}{\partial z} + b_3 T = 0 \qquad z=0 \tag{3c}$$

$$a_4 \frac{\partial T}{\partial z} + b_4 T = f(y) \qquad z=\ell_2 \tag{3d}$$

Here a_j ($j=1,2,3,4$) are conductivities, for the respective directions, and b_j are referred to as the coefficients of surface heat transfer. Through appropriate selections of the constant ratio b_j/a_j in Eqs. (3a-d), the various types of ordinary boundary conditions (prescribed temperature, heat input, and exposure to an ambient temperature through a boundary conductance) can be obtained. Equations (3a-c) correspond to zero surface temperature or heat flow on the edges $y=0$, $y=\ell_1$, and $z=0$, whereas the nonhomogeneous boundary condition of Eq. (3d) is for an arbitrary variation $f(y)$ of surface conditions along the edge $z=\ell_2$.

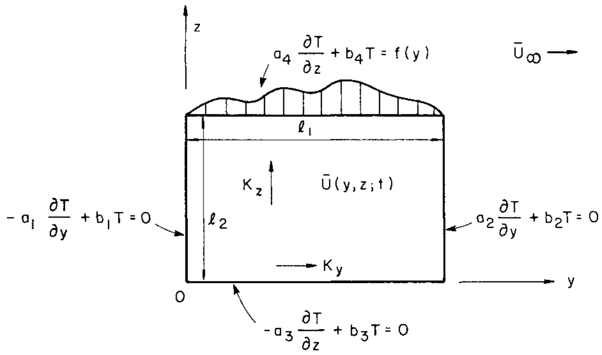

Fig. 1 An orthotropic elastic slab.

The nonhomogeneity of the boundary condition, Eq. (3d), suggests use of the principle of superposition. Noting that the problem has a steady-state solution as $t\to\infty$, we assume

$$T(y,z;t) = \phi(y,z) + \psi(y,z;t) \tag{4}$$

such that $\phi(y,z)$ and $\psi(y,z;t)$ satisfy

$$\frac{\partial^2 \phi}{\partial y^2} + K^2 \frac{\partial^2 \phi}{\partial z^2} = 0 \tag{5}$$

$$-a_1 \frac{\partial \phi}{\partial y} + b_1 \phi = 0 \qquad \text{for } y=0 \tag{6a}$$

$$a_2 \frac{\partial \phi}{\partial y} + b_2 \phi = 0 \qquad y=\ell_1 \tag{6b}$$

$$-a_3 \frac{\partial \phi}{\partial z} + b_3 \phi = 0 \qquad z=0 \tag{6c}$$

$$a_4 \frac{\partial \phi}{\partial z} + b_4 \phi = f(y) \qquad z=\ell_2 \tag{6d}$$

and

$$\frac{\partial^2 \psi}{\partial y^2} + K^2 \frac{\partial^2 \psi}{\partial z^2} = \frac{1}{D}\frac{\partial \psi}{\partial t} \tag{7}$$

$$\psi(y,z;0) = -\phi(y,z) \quad \text{for } t=0 \tag{8}$$

$$-a_1 \frac{\partial \psi}{\partial y} + b_1 \psi = 0 \quad \text{for } y=0 \tag{9a}$$

$$a_2 \frac{\partial \psi}{\partial y} + b_2 \psi = 0 \qquad y=\ell_1 \tag{9b}$$

$$-a_3 \frac{\partial \psi}{\partial z} + b_3 \psi = 0 \qquad z=0 \tag{9c}$$

$$a_4 \frac{\partial \psi}{\partial z} + b_4 \psi = 0 \qquad z=\ell_2 \tag{9d}$$

A general form of the solution of Eq. (5) is

$$\phi(y,z) = \sum_{p=p_1}^{\infty} \Big[A_1(p)\sin py \sinh\frac{pz}{K} + A_2(p)\sin py \cosh\frac{pz}{K} + A_3(p)\cos py \sinh\frac{pz}{K} + A_4(p)\cos py \cosh\frac{pz}{K} \Big] \tag{10}$$

Also, a general form of the solution to Eq. (7) is

$$\psi(y,z;t)=\sum_{\nu=\nu_1}^{\infty}\sum_{\mu=\mu_1}^{\infty}\Big(\bar{A}_1(\nu,\mu)\sin\nu y\sin\frac{\mu}{K}z+\bar{A}_2(\nu,\mu)\sin\nu y\cos\frac{\mu}{K}z+\bar{A}_3(\mu,\nu)\cos\nu y\sin\frac{\mu}{K}z+\bar{A}_4(\nu,\mu)\cos\nu y\cos\frac{\mu}{K}z\Big)\exp[-D(\nu^2+\mu^2)t] \tag{11}$$

Here, the coefficients $A_j(p)$, $\bar{A}_j(\nu,\mu)$ $(j=1,2,3,4)$, and the roots p, ν, and μ are determined from Eqs. (6), (8), and (9).

Substitution of the solutions (10) and (11) into Eqs. (6) and (9) leads, respectively, to the following results:

$$\begin{cases}-pa_1A_1(p)+b_1A_3(p)=0\\-pa_1A_2(p)+b_1A_4(p)=0\end{cases} \tag{12a}$$

$$\begin{cases}[a_2pA_1(p)+b_2A_3(p)]\cos p\ell_1+[-a_2pA_3(p)+b_2A_1(p)]\sin p\ell_1=0\\ [a_2pA_2(p)+b_2A_4(p)]\cos p\ell_1+[-a_2pA_4(p)+b_2A_2(p)]\sin p\ell_1=0\end{cases} \tag{12b}$$

$$\begin{cases}-a_3\dfrac{p}{K}A_1(p)+b_3A_2(p)=0\\ -a_3\dfrac{p}{K}A_3(p)+b_3A_4(p)=0\end{cases} \tag{12c}$$

$$\begin{aligned}f(y)=\sum_{p=p_1}^{\infty}\Big[&\Big(a_4\frac{p}{K}A_1(p)+b_4A_2(p)\Big)\cosh\frac{p}{K}\ell_2+\Big(a_4\frac{p}{K}A_2(p)+b_4A_1(p)\Big)\sinh\frac{p}{K}\ell_2\Big]\sin py\\ +\Big[&\Big(a_4\frac{p}{K}A_3(p)+b_4A_4(p)\Big)\cosh\frac{p}{K}\ell_2+\Big(a_4\frac{p}{K}A_4(p)+b_4A_3(p)\Big)\sinh\frac{p}{K}\ell_2\Big]\cos py\end{aligned} \tag{12d}$$

and

$$\begin{cases}-a_1\nu\bar{A}_1(\nu,\mu)+b_1\bar{A}_3(\nu,\mu)=0\\-a_1\nu\bar{A}_2(\nu,\mu)+b_1\bar{A}_4(\nu,\mu)=0\end{cases} \tag{13a}$$

$$\begin{cases}[a_2\nu\bar{A}_1(\nu,\mu)+b_2\bar{A}_3(\nu,\mu)]\cos\nu\ell_1+[-a_2\nu\bar{A}_3(\nu,\mu)+b_2\bar{A}_1(\nu,\mu)]\sin\nu\ell_1=0\\ [a_2\nu\bar{A}_2(\nu,\mu)+b_2\bar{A}_4(\nu,\mu)]\cos\nu\ell_1+[-a_2\nu\bar{A}_4(\nu,\mu)+b_2\bar{A}_2(\nu,\mu)]\sin\nu\ell_1=0\end{cases} \tag{13b}$$

$$\begin{cases}-a_3\dfrac{\mu}{K}\bar{A}_1(\nu,\mu)+b_3\bar{A}_2(\nu,\mu)=0\\ -a_3\dfrac{\mu}{K}\bar{A}_3(\nu,\mu)+b_3\bar{A}_4(\nu,\mu)=0\end{cases} \tag{13c}$$

$$\begin{cases}\Big[a_4\dfrac{\mu}{K}\bar{A}_1(\nu,\mu)+b_4\bar{A}_2(\nu,\mu)\Big]\cos\dfrac{\mu}{K}\ell_2+\Big[-a_4\dfrac{\mu}{K}\bar{A}_2(\nu,\mu)+b_4\bar{A}_1(\nu,\mu)\Big]\sin\dfrac{\mu}{K}\ell_2=0\\ \Big[a_4\dfrac{\mu}{K}\bar{A}_3(\nu,\mu)+b_4\bar{A}_4(\nu,\mu)\Big]\cos\dfrac{\mu}{K}\ell_2+\Big[-a_4\dfrac{\mu}{K}\bar{A}_4(\nu,\mu)+b_4\bar{A}_3(\nu,\mu)\Big]\sin\dfrac{\mu}{K}\ell_2=0\end{cases} \tag{13d}$$

The solution of Eqs. (12) and (13) for the coefficients $A_j(p)$ and $\bar{A}_j(\nu,\mu)$ $(j=1,2,3,4)$ is simplified if the attention is restricted to a specific set of boundary conditions for the three edges $y=0$, $y=\ell_1$, $z=0$.

As the first example, we consider the case where the three edges $y=0$, $y=\ell_1$, and $z=0$ are held at the constant temperature $T=0$ (i.e., $a_1=a_2=a_3=0$, $b_1=b_2=b_3=1$). Substituting these choices of a_j and b_j into Eqs. (12a-c) yields

$$A_1(p)\sin p\ell_1=A_2(p)=A_3(p)=A_4(p)=0 \tag{14}$$

Thus, for a nontrivial solution of $\phi(y,z)$,

$$p_n=\frac{n\pi}{\ell_1},\quad n=1,2,\ldots,\infty \tag{15}$$

and Eq. (12d) reduces to

$$f(y)=\sum_{n=1}^{\infty}\Big[a_4\frac{p_n}{K}\cosh\frac{p_n}{K}\ell_2+b_4\sinh\frac{p_n}{K}\ell_2\Big]A_1(p_n)\sin p_ny \tag{16}$$

Assuming that the distribution $f(y)$ may be expressed in the Fourier series form

$$f(y)=\sum_{n=1}^{\infty}Q_n\sin\frac{n\pi}{\ell_1}y \tag{17}$$

in which

$$Q_n=\frac{2}{\ell_1}\int_0^{\ell_1}f(y)\sin\frac{n\pi}{\ell_1}y\,dy$$

it follows from Eq. (16) that

$$\phi(y,z)=\sum_{n=1}^{\infty}A_1(p_n)\sin p_ny\sinh\frac{p_n}{K}z \tag{18}$$

where

$$A_1(p_n)=\frac{\dfrac{2}{\ell_1}\displaystyle\int_0^{\ell_1}f(y)\sin p_ny\,dy}{a_4\dfrac{p_n}{K}\cosh\dfrac{p_n\ell_2}{K}+b_4\sinh\dfrac{p_n\ell_2}{K}}$$

On the other hand, substituting the same choice of a_j and b_j as above into Eqs. (13a-d) yields

$$\bar{A}_1(\nu,\mu)\sin\nu\ell_1=\bar{A}_2(\nu,\mu)=\bar{A}_3(\nu,\mu)=\bar{A}_4(\nu,\mu)=0 \tag{19}$$

Thus, for a nontrivial solution of $\psi(y,z;t)$

$$\nu_k=\frac{k\pi}{\ell_1},\quad k=1,2,\ldots,\infty \tag{20}$$

and $(\mu/k)\ell_2$ are the positive roots of the equation

$$\left(\frac{\mu}{K}\ell_2\right)\cot\left(\frac{\mu}{K}\ell_2\right)+\frac{b_4}{a_4}\ell_2=0 \tag{21}$$

These roots can be found in standard reference books, such as Ref. 11. Using the initial condition, Eq. (8), we obtain

$$\psi(y,z;0)=-\phi(y,z)=\sum_{k=1}^{\infty}\sum_{m=1}^{\infty}\bar{A}_1(\nu_k,\mu_m)\sin\nu_k y\sin\frac{\mu_m}{K}z \tag{22}$$

Thus, $\psi(y,z;0)$ is the expansion of $-\phi(y,z)$ into a double Fourier series. Here the coefficient $\bar{A}_1(\nu_k,\mu_m)$ is

$$\bar{A}_1(\nu_k,\mu_m)=\frac{\int_0^{\ell_1}\int_0^{\ell_2}[-\phi(y,z)]\sin\nu_k y\sin\frac{\mu_m}{K}z\,dy\,dz}{\int_0^{\ell_1}\int_0^{\ell_2}\sin^2\nu_k y\sin^2\frac{\mu_m}{K}z\,dy\,dz} \tag{23}$$

By substitution of Eq. (18) into Eq. (23) and evaluating the inner integrals, we can obtain the expression of $\bar{A}_1(\nu_k,\mu_m)$.

Finally, the transient temperature distribution for this example is

$$T(y,z;t)=\sum_{k=1}^{\infty}A_{k,1}(\nu_k)\sin\nu_k y\sinh\frac{\nu_k}{K}z+\sum_{k=1}^{\infty}\sum_{m=1}^{\infty}\bar{A}_{km,1}(\nu_k,\mu_m)\sin\nu_k y\sin\frac{\mu_m}{K}z\exp[-D(\nu_k^2+\mu_m^2)t] \tag{24}$$

where

$$\bar{A}_{km,1}(\nu_k,\mu_m)=\frac{-2}{\ell_2}\frac{A_{k,1}(\nu_k)}{\left(\frac{\nu_k}{K}\right)^2+\left(\frac{\mu_m}{K}\right)^2}\times\left[\frac{\nu_k}{K}\cosh\frac{\nu_k}{K}\ell_2\sin\frac{\mu_m}{K}\ell_2-\frac{\mu_m}{K}\sinh\frac{\nu_k}{K}\ell_2\cos\frac{\mu_m}{K}\ell_2\right]$$

$$A_{k,1}=\frac{\frac{2}{\ell_1}\int_0^{\ell_1}f(y)\sin\nu_k y\,dy}{a_4\frac{\nu_k}{K}\cosh\frac{\nu_k}{K}\ell_2+b_4\sinh\frac{\nu_k}{K}\ell_2}$$

and in the particular case of $a_4=0$ and $b_4=1$, we have

$$\frac{\mu_m}{K}\ell_2=m\pi=\alpha_m$$

Equation (24) will be used in Sec. IV for its induced thermal stress calculations.

As the second example, we consider the problem of perfect insulation on the three edges ($y=0$, $y=\ell_1$, and $z=0$), in which case $a_1=a_2=a_3=1$, $b_1=b_2=b_3=0$, and the condition at $z=\ell_2$ remains unchanged [i.e., $a_4(\partial T/\partial z)+b_4T=f(y)$]. Following the same approach as the first example, we obtain

$$A_1(p)=A_2(p)=A_3(p)=A_4\sin p\ell_1=0 \tag{25}$$

Thus, for a nontrivial solution of $\phi(y,z)$

$$p_n=n\pi/\ell_1,\quad n=1,2,\ldots,\infty \tag{26}$$

and

$$\bar{A}_1(\nu,\mu)=\bar{A}_2(\nu,\mu)=\bar{A}_3(\nu,\mu)=\bar{A}_4\sin\nu\ell_1=0 \tag{27}$$

μ_m are the positive roots of Eq. (28)

$$\left(\frac{\mu}{K}\ell_2\right)\tan\left(\frac{\mu}{K}\ell_2\right)=\frac{b_4}{a_4}\ell_2 \tag{28}$$

The temperature field is given by

$$T(y,z;t)=\sum_{k=1}^{\infty}A_{k,4}(\nu_k)\cos\nu_k y\cosh\frac{\nu_k}{K}z+\sum_{k=1}^{\infty}\sum_{m=1}^{\infty}\bar{A}_{km,4}(\nu_k,\mu_m)\cos\nu_k y\cos\frac{\mu_m}{K}z\exp[-D(\nu_k^2+\mu_m^2)t] \tag{29}$$

where

$$\bar{A}_{km,4}=\frac{-2}{\ell_2}\frac{A_{k,4}(\nu_k)}{\left(\frac{\nu_k}{K}\right)^2+\left(\frac{\mu_m}{K}\right)^2}\times\left[\frac{\nu_k}{K}\sinh\frac{\nu_k}{K}\ell_2\cos\frac{\mu_m}{K}\ell_2+\frac{\mu_m}{K}\cosh\frac{\nu_k}{K}\ell_2\sin\frac{\mu_m}{K}\ell_2\right]$$

$$A_{k,4}=\frac{\frac{2}{\ell_1}\int_0^{\ell_1}f(y)\cos\nu_k y\,dy}{a_4\frac{\nu_k}{K}\sinh\frac{\nu_k}{K}\ell_2+b_4\cosh\frac{\nu_k}{K}\ell_2}$$

$$\nu_k=k\pi/\ell_1$$

Analytical results for other combinations of boundary conditions can also be obtained following the approach demonstrated in the last two examples [Eqs. (24) and (29)]. In Appendix 1, the results for eight types of boundary conditions from all the possible combinations of a_1, a_2, a_3, b_1, b_2, b_3 are tabulated for convenient use.

For problems involving nonhomogeneous boundary conditions over more than one edge, solutions of the temperature can be obtained from the present results by means of appropriate coordinate transformations and the method of superposition.

III. Thermal Stress Field

As an application of the foregoing temperature distribution $T(y,z;t)$, we now consider the induced thermal stress field in the orthotropic slab. For a state of plane-strain perpendicular to the x axis ($\epsilon_{xx}=\epsilon_{zx}=\epsilon_{xy}=0$), the displacement components in the x, y, and z directions are, respectively, $u=0$, $v=v(y,z;t)$, and $w=w(y,z;t)$. The stress components are related to the displacements and temperature by the relationships

$$\sigma_{xx}(y,z;t)=A_{12}\frac{\partial v}{\partial y}+A_{13}\frac{\partial w}{\partial z}-\beta_1T(y,z;t)$$

$$\sigma_{yy}(y,z;t)=A_{22}\frac{\partial v}{\partial y}+A_{23}\frac{\partial w}{\partial z}-\beta_2T(y,z;t)$$

$$\sigma_{zz}(y,z;t)=A_{23}\frac{\partial v}{\partial y}+A_{33}\frac{\partial w}{\partial z}-\beta_3T(y,z;t)$$

$$\sigma_{yz}(y,z;t)=A_{44}\left(\frac{\partial v}{\partial z}+\frac{\partial w}{\partial y}\right) \tag{30}$$

where A_{ij} and β_i are, respectively, the elastic stiffness coefficients and stress/temperature coefficients of the orthotropic elastic medium. Results for the corresponding plane-stress problem ($\sigma_{xx} = \sigma_{xy} = \sigma_{xz} = 0$) can be obtained by replacing the coefficients A_{ij} and β_i by $A_{ij} - A_{1i}A_{1j}/A_{11}$ and $\beta_i - \beta_1 A_{1i}/A_{11}$, respectively. The displacement equations of equilibrium governing the plane-strain conditions are

$$A_{22}\frac{\partial^2 v}{\partial y^2} + A_{44}\frac{\partial^2 v}{\partial z^2} + (A_{23}+A_{44})\frac{\partial^2 w}{\partial y \partial z} = \beta_2 \frac{\partial T}{\partial y}$$
$$A_{44}\frac{\partial^2 w}{\partial y^2} + A_{33}\frac{\partial^2 w}{\partial z^2} + (A_{23}+A_{44})\frac{\partial^2 v}{\partial y \partial z} = \beta_3 \frac{\partial T}{\partial z} \quad (31)$$

The stress and displacement boundary conditions are assumed for this problem. The transverse displacement and the longitudinal stress vanish at the two edges of the rectangular slab, $y=0$ and $y=\ell_1$; the two other edges, $z=0$ and $z=\ell_2$, are stress-free. Thus,

$$w=0, \quad \sigma_{yy}=0 \quad \text{for } y=0,\ell_1 \quad (32a)$$

$$\sigma_{zz}=0, \quad \sigma_{yz}=0 \qquad z=0,\ell_2 \quad (32b)$$

The displacement-potential approach, reported recently by Wang and Chou,[11] is adopted for the thermal stress analysis. As an example, we consider the case where the temperature field $T(y,z;t)$ is given by Eq. (24). It can be shown that the solution to Eqs. (31) for this case, satisfying the boundary condition of Eq. (32a), is

$$v(y,z;t) = \frac{\partial \Psi_1}{\partial y} + \frac{\partial \Psi_2}{\partial y} + \frac{\partial \Phi_1}{\partial y} + \frac{\partial \Phi_2}{\partial y}$$
$$w(y,z;t) = \mu_1 \frac{\partial \Psi_1}{\partial z} + \mu_2 \frac{\partial \Psi_2}{\partial z} + \lambda_1 \frac{\partial \Phi_1}{\partial z} + \lambda_2 \frac{\partial \Phi_2}{\partial z} \quad (33)$$

where

$$\Psi_1 = \sum_{k=1}^{\infty} A_{k,1} B_k \sin\nu_k y \sinh \frac{\nu_k}{K} z \quad (34)$$

$$\Psi_2 = \sum_{k=1}^{\infty}\sum_{m=1}^{\infty} \bar{A}_{km,1} B_{km} \sin\nu_k y \sin\alpha_m z \exp[-D(\nu_k^2 + K^2\alpha_m^2)t] \quad (35)$$

$$\Phi_j = \sum_{k=1}^{\infty}\left(C_{j1}\sin\nu_k y \sinh\frac{\nu_k}{\gamma_j}z + C_{j2}\sin\nu_k y\cosh\frac{\nu_k}{\gamma_j}z\right) \quad (36)$$
$$(j=1,2)$$

C_{ij} $(j,i=1,2)$ in Eq. (36) are arbitrary coefficients. Other constants appearing in Eqs. (33-36) are

$$\mu_1 = \frac{\beta_3(A_{44} - A_{22}K^2) + \beta_2 K^2 (A_{23}+A_{44})}{\beta_2(A_{33} - A_{44}K^2) - \beta_3(A_{23}+A_{44})} \quad (37)$$

$$B_k \nu_k^2 = \frac{\beta_2 K^2}{-A_{22}K^2 + A_{44} + \mu_1(A_{23}+A_{44})} \quad (38)$$

$$\mu_2 = \frac{-\beta_3(A_{22}\nu_k^2 + A_{44}\alpha_m^2) + \beta_2(A_{23}+A_{44})\nu_k^2}{\beta_3(A_{23}+A_{44})\alpha_m^2 - \beta_2(A_{44}\nu_k^2 + A_{33}\alpha_m^2)} \quad (39)$$

$$B_{km} = \frac{-\beta_2}{A_{22}\nu_k^2 + [A_{44} + \mu_2(A_{23}+A_{44})]\alpha_m^2} \quad (40)$$

$$\gamma_k^2 = \frac{A_{44} + \lambda_k(A_{23}+A_{44})}{A_{22}}, \quad (k=1,2) \quad (41)$$

where

$$\lambda_{1,2} = \frac{-1}{2}\rho \pm \sqrt{\left(\frac{\rho}{2}\right)^2 - 1} \quad (42)$$

with

$$\rho = \frac{(A_{23}+A_{44})^2 + A_{44}^2 - A_{22}A_{33}}{A_{44}(A_{23}+A_{44})}$$

Following Eqs. (33) and (30), the displacement and stress components are

$$v(y,z;t) = \sum_{k=1}^{\infty} \nu_k \Bigg[C_{11}\sinh\frac{\nu_k}{\gamma_1}z + C_{12}\cosh\frac{\nu_k}{\gamma_1}z + C_{21}\sinh\frac{\nu_k}{\gamma_2}z + C_{22}\cosh\frac{\nu_k}{\gamma_2}z + A_{k,1}B_k\sinh\frac{\nu_k}{K}z + \sum_{m=1}^{\infty}\bar{A}_{km,1}B_{km}\sin\alpha_m z\exp[-D(\nu_k^2+K^2\alpha_m^2)t]\Bigg]\cos\nu_k y$$

$$w(y,z;t) = \sum_{k=1}^{\infty}\Bigg[\mu_1\frac{\nu_k}{K}A_{k,1}B_k\cosh\frac{\nu_k}{K}z + \lambda_1\frac{\nu_k}{\gamma_1}\left(C_{11}\cosh\frac{\nu_k}{\gamma_1}z + C_{12}\sinh\frac{\nu_k}{\gamma_1}z\right) + \lambda_2\frac{\nu_k}{\gamma_2}\left(C_{21}\cosh\frac{\nu_k}{\gamma_2}z + C_{22}\sinh\frac{\nu_k}{\gamma_2}z\right) + \sum_{m=1}^{\infty}\mu_2\alpha_m\bar{A}_{km,1}B_{km}\cos\alpha_m z\exp[-D(\nu_k^2+K^2\alpha_m^2)t]\Bigg]\sin\nu_k y$$
$$(43)$$

$$\sigma_{xx} = \sum_{k=1}^{\infty}\Bigg[\alpha_k^2E_{11}\left(C_{11}\sinh\frac{\nu_k}{\gamma_1}z + C_{12}\cosh\frac{\nu_k}{\gamma_1}z\right) + \alpha_k^2E_{12}\left(C_{21}\sinh\frac{\nu_k}{\gamma_2}z + C_{22}\cosh\frac{\nu_k}{\gamma_2}z\right) + A_{k,1}(\alpha_k)E_{13}\sinh\frac{\nu_k}{K}z + \sum_{m=1}^{\infty}\bar{A}_{km,1}(\nu_k,\alpha_m)E_{14}\sin\alpha_m z \times\exp[-D(\nu_k^2+K^2\alpha_m^2)t]\Bigg]\sin\nu_k y$$

$$\sigma_{yy} = \sum_{k=1}^{\infty}\Bigg[\nu_k^2E_{21}\left(C_{11}\sinh\frac{\nu_k}{\gamma_1}z + C_{12}\cosh\frac{\nu_k}{\gamma_1}z\right) + \nu_k^2E_{22}\left(C_{21}\sinh\frac{\nu_k}{\gamma_2}z + C_{22}\cosh\frac{\nu_k}{\gamma_2}z\right) + A_{k,1}(\nu_k)E_{23}\sinh\frac{\nu_k}{K}z + \sum_{m=1}^{\infty}\bar{A}_{km,1}(\nu_k,\alpha_m)E_{24}\sin\alpha_m z \times\exp[-D(\nu_k^2+K^2\alpha_m^2)t]\Bigg)\sin\nu_k y$$

$$\sigma_{zz} = \sum_{k=1}^{\infty}\Bigg[\nu_k^2E_{31}\left(C_{11}\sinh\frac{\nu_k}{\gamma_1}z + C_{12}\cosh\frac{\nu_k}{\gamma_1}z\right) + \nu_k^2E_{32}\left(C_{21}\sinh\frac{\nu_k}{\gamma_2}z + C_{22}\cosh\frac{\nu_k}{\gamma_2}z\right) + A_{k,1}(\nu_k)E_{33}\sinh\frac{\nu_k}{K}z + \sum_{m=1}^{\infty}\bar{A}_{km,1}(\nu_k,\alpha_m)E_{34}\sin\alpha_m z \times\exp[-D(\nu_k^2+K^2\alpha_m^2)t]\Bigg]\sin\nu_k y$$

$$\sigma_{yz}=\sum_{k=1}^{\infty}\left[\nu_k^2E_{41}\left(C_{11}\cosh\frac{\nu_k}{\gamma_1}z+C_{12}\sinh\frac{\nu_k}{\gamma_1}z\right)\right.$$
$$+\nu_k^2E_{42}\left(C_{21}\cosh\frac{\nu_k}{\gamma_2}z+C_{22}\sinh\frac{\nu_k}{\gamma_2}z\right)$$
$$+A_{k,1}E_{43}\cosh\frac{\nu_k}{K}z$$
$$\left.+\sum_{m=1}^{\infty}\bar{A}_{km,1}E_{44}\cos\alpha_m z\exp[-D(\nu_k^2+K^2\alpha_m^2)t]\right]\cos\nu_k y \tag{44}$$

where the quantities E_{jk} are

$$E_{jk}=-A_{j2}+\frac{\lambda_k}{\gamma_k^2}A_{j3},\quad (j=2,3\ \ k=1,2)$$

$$E_{j3}=-A_{j2}\nu_k^2B_k+\frac{\mu_1}{K^2}\nu_k^2B_kA_{j3}-\beta_j,\quad (j=1,2,3)$$

$$E_{j4}=-A_{j2}\nu_k^2B_{km}-\mu_2A_{j3}\alpha_m^2B_{km}-\beta_j,\quad (j=1,2,3)$$

$$E_{4k}=A_{44}(1+\lambda_k)/\gamma_k,\quad (k=1,2)$$

$$E_{43}=A_{44}(1+\mu_1)\frac{\nu_k^2B_k}{K}$$

$$E_{44}=A_{44}(1+\mu_2)\nu_k\alpha_mB_{km}$$

The coefficients C_{ij} $(i=1,2,\ j=1,2)$ are found from the four boundary conditions, Eq. (32b).

IV. Illustrative Example and Discussion

To illustrate the foregoing analysis of temperature and the induced thermal stress fields, a numerical example is presented for a slab constructed of a fiber-reinforced composite material, with fibers oriented parallel to the y axis (Fig. 2). The same thermal and elastic properties as given in Ref. 15 are adopted for our numerical calculation in order to demonstrate the transient effects.

$$K_z/K_y=0.1,\qquad \beta_1=124\ \text{psi}/^\circ\text{F}$$
$$\beta_2=204\ \text{psi}/^\circ\text{F},\qquad \beta_3=118\ \text{psi}/^\circ\text{F}$$
$$A_{22}=30.3\times10^6\ \text{psi},\quad A_{33}=4.04\times10^6\ \text{psi}$$
$$A_{44}=1.13\times10^6\ \text{psi},\quad A_{23}=3.78\times10^6\ \text{psi}$$
$$A_{13}=1.99\times10^6\ \text{psi},\quad A_{12}=3.35\times10^6\ \text{psi} \tag{45}$$

The initial temperature of the slab is $T=0$, then a temperature rise of the form $T=T_0\sin(\pi/\ell_1)y$ is assumed to exist over the top edge $(z=\ell_2)$ of the slab, while the temperature over the remainder of the boundary is maintained at the initial value. So, in our case, the temperature distribution solution, Eq. (24), is applicable if we take

$$a_4=0,\quad b_4=1$$

$$f(y)=T_0\sin\frac{\pi}{\ell_1}y \tag{46}$$

If the faces $z=0$ and ℓ_2 are assumed to be traction-free, the mechanical boundary condition is given by Eq. (32b). Since the temperature rise $f(y)$ in Eq. (46) is represented by a Fourier series with a single harmonic, it is sufficient in the present example to consider only the first term of its series representations for the temperature [Eq. (24)] and stresses [Eq. (44)], i.e., $k=1$ in these equations. On the other hand, the time-dependent parts of the Fourier series in Eqs. (24) and (44), i.e., $\sum_{m=1}^{\infty}$, are determined at each of the prescribed time intervals by evaluating the first 20 terms of the infinite series, i.e., $m=20$. The numerical results for $\ell_2/\ell_1=0.25$ show less than 1% change when 40 terms are included in the series calculation.

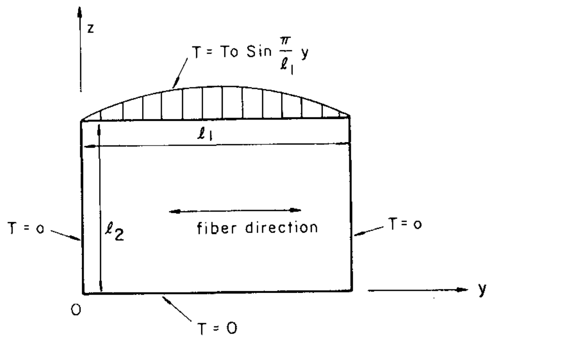

Fig. 2 Geometry and thermal boundary conditions used in the illustrative example.

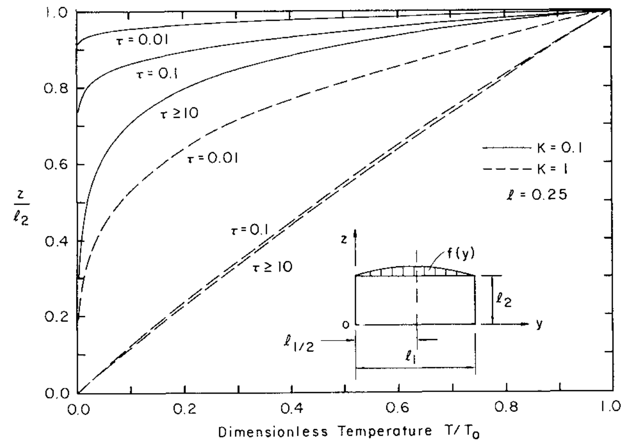

a) At $y=\ell_1/2$.

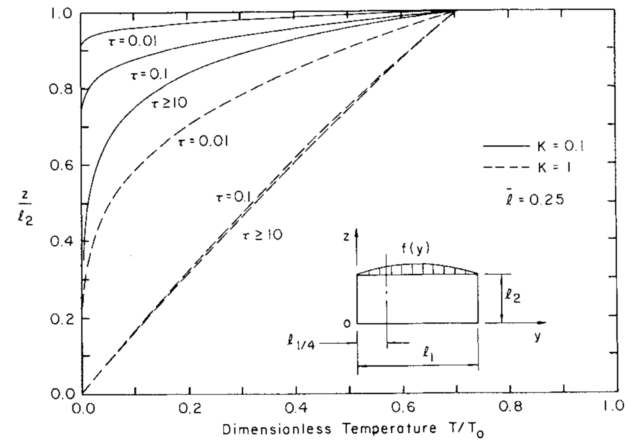

b) At $y=\ell_1/4$.

Fig. 3 Transient temperature distributions for $K=1.0$ and 0.1.

For the convenience of presenting the numerical results, the following dimensionless quantities are introduced for temperature, stress, time, and geometry, respectively.

$$\bar{T}=T(y,z;t)/T_0,\quad \bar{\sigma}_{ij}=\sigma_{ij}(y,Z;t)/\beta_3T_0,\quad \tau=Dt/\ell_1^2,\quad \bar{\ell}=\ell_2/\ell_1$$

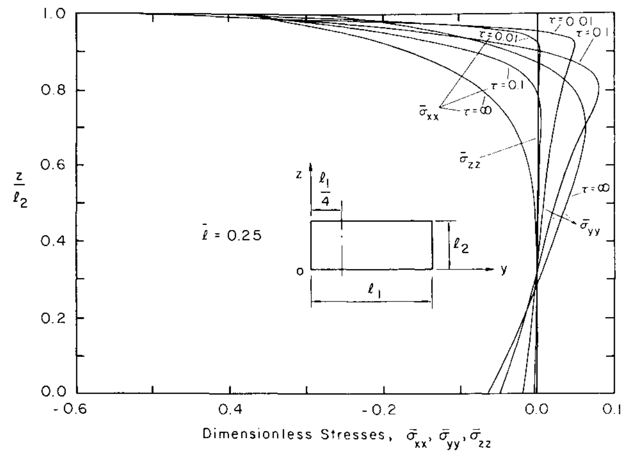

a) **Normal stress.**

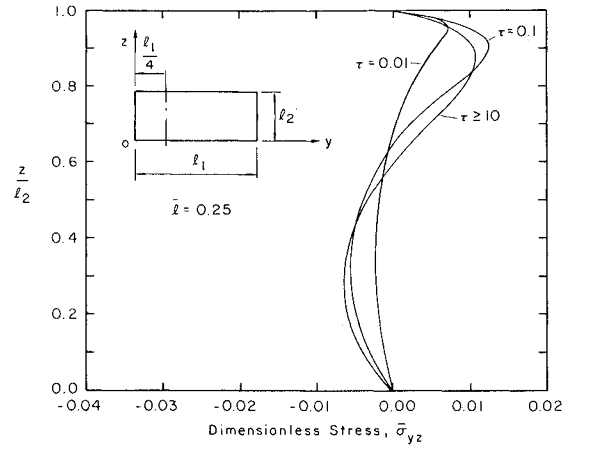

b) **Shear stress.**

Fig. 4 Transient thermal stress distributions for $K=0.1$ at the cross section $y=\ell_1/4$.

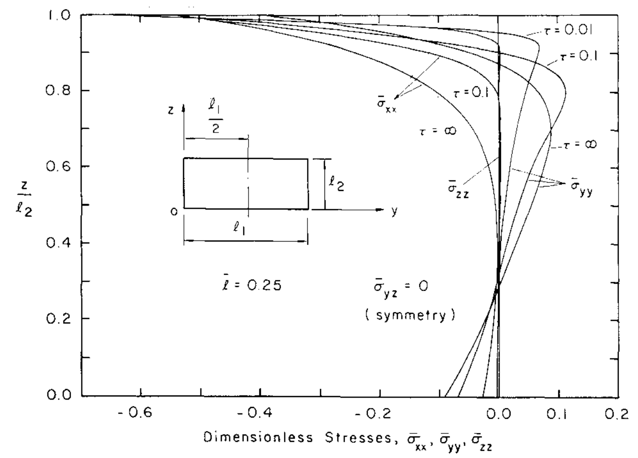

Fig. 5 Transient thermal stress distributions for $K=0.1$ at the cross section $y=\ell_1/2$.

Figures 3a and 3b show, respectively, the z direction temperature distribution at the cross sections, $y=\ell_1/4$ and $y=\ell_1/2$ for the various dimensionless time intervals. For the purpose of comparison, dashed lines denote results for an isotropic material (i.e., $K=1$). The temperature gradient, $\partial T/\partial z$, at the heated upper edge of the rectangle increases with an increasing degree of orthotropy.

Figures 4a, 4b, and 5 show the z direction variation of thermal stresses at cross sections $y=\ell_1/4$ and $y=\ell_1/2$, respectively, for the various dimensionless time intervals. It is clear

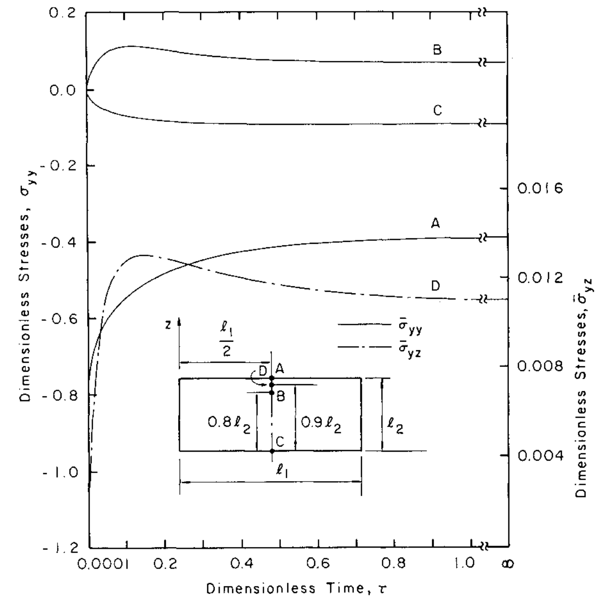

Fig. 6 Thermal stresses as a function of the dimensionless time for $K=0.1$ at the location A, B, C, and D of the cross section $y=\ell_1/2$.

that large longitudinal stress σ_{yy} occurs in the vicinity of the heated boundary where the relatively large temperature gradient $\partial T/\partial z$ exists. In the meantime, the transverse stress σ_{zz} and the shear stress σ_{yz} are relatively small. Also, for σ_{yy} the maximum transient tensile stress is 28% higher than that in the steady-state; the maximum transient compressive stress near the upper edge ($z=\ell_2$) is 82% higher than that in the steady-state. Figure 6 shows the time dependence of thermal stresses at points A, B, C, and D of the cross section $y=\ell_1/2$.

The effect of length to width ratio of the rectangular slab, $\bar{\ell}$, on the longitudinal stress distributions also have been examined. It has been found that the maximum transient tensile stress is 25-66% higher, and the maximum transient compressive stress is 58-162% higher than the corresponding steady-state values for $\bar{\ell}=0.125 \sim 0.5$.

An examination of the plots of σ_{yy}, σ_{zz}, and σ_{yz} at any given time interval indicates that each stress is in self-equilibrium. This is consistent with the nature of thermal residual stresses.

V. Conclusions

1) A two-dimensional thermal transient problem for a thermally and elastically orthotropic material has been solved. The elastic medium assumes the shape of a rectangle with one of its edges subjected to an instantaneous variation in temperature, heat flow, or convection, while each of the remaining edges is either insulated or maintained at the initial temperature. General solutions in closed form for the temperature distribution are obtained based on the solution of the classical diffusion equation. The temperature solutions for various combinations of boundary conditions are tabulated for convenient use. Exact thermal stress solutions are determined by the use of a displacement-potential approach. Both the temperature and stress solutions are presented in series form.

2) For problems involving nonhomogeneous initial conditions [i.e., $t=0$, $T(y,z,0)=f(y,z)$] and homogeneous boundary conditions on all edges of the slab (i.e., $T=0$ or $\partial T/\partial n=0$ for $y=0,\ell_1$, $z=0,\ell_2$), solutions can also be obtained based on the information in Table 1. This will be discussed in a separate article.

3) The thermal orthotropy has significant influence on the temperature and thermal stress distributions in the elastic

Table 1 Temperature coefficients $A_{k,j}$ and $\bar{A}_{km,j}$ corresponding to various boundary conditions

Case	Boundary conditions	$\bar{A}_{km,j}(\nu,\mu)$ $(j=1,2,3,4)$	$A_{k,j}(\nu)$ $(j=1,2,3,4)$	p_k, ν_k	Eqs. for μ
1	$a_1=a_2=a_3=0$	$\bar{A}_{km,2}=\bar{A}_{km,3}=\bar{A}_{km,4}=0$	$A_{k,2}=A_{k,3}=A_{k,4}=0$		
	$b_1=b_2=b_3=1$	$A_{km,1}=\dfrac{-2A_{k,1}}{\ell_2}G_1(\nu,\mu)$	$A_{k,1}=\dfrac{2}{\ell_1 g_1(\nu)}\int_0^{\ell_1}f(y)\sin\nu y dy$	$\dfrac{k\pi}{\ell_1}$	Eq. (A5)
	$f(y)=\sum_{n=1}^{\infty}P_n\sin\dfrac{n\pi y}{\ell_1}$				
2	$a_1=a_2=b_3=0$	$\bar{A}_{km,1}=\bar{A}_{km,3}=\bar{A}_{km,4}=0$	$A_{k,1}=A_{k,3}=A_{k,4}=0$		
	$b_1=b_2=a_3=1$	$\bar{A}_{km,2}=\dfrac{-2A_{k,2}}{\ell_2}G_2(\nu,\mu)$	$A_{k,2}=\dfrac{2}{\ell_1 g_2(\nu)}\int_0^{\ell_1}f(y)\sin\nu y dy$	$\dfrac{k\pi}{\ell_1}$	Eq. (A6)
	$f(y)=\sum_{n=1}^{\infty}P_n\sin\dfrac{n\pi y}{\ell_1}$				
3	$a_1=a_3=b_2=0$	$\bar{A}_{km,2}=\bar{A}_{km,3}=\bar{A}_{km,4}=0$	$A_{k,2}=A_{k,3}=A_{k,4}=0$		
	$b_1=b_3=a_2=0$	$\bar{A}_{km,1}=\dfrac{-2A_{k,1}}{\ell_2}G_1(\nu,\mu)$	$A_{k,1}=\dfrac{2}{\ell_1 g_1(\nu)}\int_0^{\ell_1}f(y)\sin\nu y dy$	$\dfrac{2k-1}{2\ell_1}\pi$	Eq. (A5)
	$f(y)=\sum_{n=1}^{\infty}P_n\sin\dfrac{(2n-1)}{2\ell_1}\pi y$				
4	$a_1=b_2=b_3=0$	$\bar{A}_{km,1}=\bar{A}_{km,3}=\bar{A}_{km,4}=0$	$A_{k,1}=A_{k,3}=A_{k,4}=0$		
	$b_1=a_2=a_3=1$	$\bar{A}_{km,2}=\dfrac{-2A_{k,2}}{\ell_2}G_2(\nu,\mu)$	$A_{k,2}=\dfrac{2}{\ell_1 g_2(\nu)}\int_0^{\ell_1}f(y)\sin\nu y dy$	$\dfrac{2k-1}{2\ell_1}\pi$	Eq. (A6)
	$f(y)=\sum_{n=1}^{\infty}P_n\dfrac{(2n-1)}{2\ell_1}\pi y$				
5	$b_1=a_2=a_3=0$	$\bar{A}_{km,1}=\bar{A}_{km,2}=\bar{A}_{km,4}=0$	$A_{k,1}=A_{k,2}=A_{k,4}=0$		
	$a_1=b_2=b_3=1$	$\bar{A}_{km,3}=\dfrac{-2A_{k,3}}{\ell_2}G_1(\nu,\mu)$	$A_{k,3}=\dfrac{2}{\ell_1 g_1(\nu)}\int_0^{\ell_1}f(y)\cos\nu y dy$	$\dfrac{2k-1}{2\ell_1}\pi$	Eq. (A5)
	$f(y)=\sum_{n=1}^{\infty}Q_n\cos\dfrac{(2n-1)}{2\ell_1}\pi y$				
6	$b_1=a_2=b_3=0$	$\bar{A}_{km,1}=\bar{A}_{km,2}=\bar{A}_{km,3}=0$	$A_{k,1}=A_{k,2}=A_{k,3}=0$		
	$a_1=b_2=a_3=1$	$\bar{A}_{km,4}=\dfrac{-2A_{k,4}}{\ell_2}G_2(\nu,\mu)$	$A_{k,4}=\dfrac{2}{\ell_1 g_2(\nu)}\int_0^{\ell_1}f(y)\cos\nu y dy$	$\dfrac{2k-1}{2\ell_1}\pi$	Eq. (A6)
	$f(y)=\sum_{n=1}^{\infty}Q_n\cos\dfrac{(2n-1)}{2\ell_1}\pi y$				
7	$b_1=b_2=a_3=0$	$\bar{A}_{km,1}=\bar{A}_{km,2}=\bar{A}_{km,4}=0$	$A_{k,1}=A_{k,2}=A_{k,4}=0$		
	$a_1=a_2=b_3=1$	$A_{km,3}=\dfrac{-2A_{k,3}}{\ell_2}G_1(\nu,\mu)$	$A_{k,3}=\dfrac{2}{\ell_1 g_1(\nu)}\int_0^{\ell_1}f(y)\cos\nu y dy$	$\dfrac{k\pi}{\ell_1}$	Eq. (A5)
	$f(y)=\sum_{n=1}^{\infty}Q_n\cos\dfrac{n\pi y}{\ell_1}$				
8	$b_1=b_2=b_3=0$	$\bar{A}_{km,1}=\bar{A}_{km,2}=\bar{A}_{km,3}=0$	$A_{k,1}=A_{k,2}=A_{k,3}=0$		
	$a_1=a_2=a_3=1$	$\bar{A}_{km,4}=\dfrac{-2A_{k,4}}{\ell_2}G_2(\nu,\mu)$	$A_{k,4}=\dfrac{2}{\ell_1 g_2(\nu)}\int_0^{\ell_1}f(y)\cos\nu y dy$	$\dfrac{k\pi}{\ell_1}$	Eq. (A6)
	$f(y)=\sum_{n=1}^{\infty}Q_n\cos\dfrac{n\pi y}{\ell_1}$				

body. Numerical experiments simulating a unidirectional fiber-reinforced composite material have been performed. The ratio of heat conductivities in the longitudinal and transverse directions is $K_z/K_y = 0.01$ and the slab geometry $\bar{\ell} = 0.125 \sim 0.5$. The results have shown that maximum transient tensile stress in the range of $125 \sim 166\%$ of those for the steady-state, maximum transient compressive stress in the range of $158 \sim 262\%$ of those for the steady-state, and maximum transient shear stress in the range of $103 \sim 160\%$ of those for the steady-state. This finding suggests the need to find the history of temperature and thermal stress variations for the practical applications of orthotropic materials. The dimensionless time constants required to reach steady-state for any given orthotropic material system can be easily calculated.

4) Since the present results have demonstrated the importance of considering the transient process in analyzing the thermal behavior of the fiber-reinforced composites and the array of problems involving, for instance, boundary-layer stress concentrations and interfacial damage of laminates under severe thermal (and hygrothermal) conditions, all deserve in-depth assessment and examination in the future.

Acknowledgments

The authors wish to thank the Center for Composite Materials of the University of Delaware for partial support. They acknowledge the support of the Office of Naval Research, Dr. L. H. Peebles Jr., Technical Monitor.

Appendix 1: Unsteady-State Temperature Distributions for Various Boundary Conditions

Following the procedure used to obtain the temperature distribution in Sec. II, solutions can be found for various other combinations of edge conditions. The eigenvalues p, ν, μ and the coefficients $A_j(\nu)$ and $\bar{A}_j(\nu,\mu)$, to be used in the temperature expressions (10) and (11), were calculated for eight different sets of boundary conditions. These results are summarized in Table 1 for convenient use. The functions $G_1(\nu,\mu)$, $G_2(\eta,\mu)$, $g_1(\nu)$, $g_2(\nu)$ and the equations of μ appearing in the table are given by

$$G_1(\nu,\mu) = \frac{1}{\left(\frac{\nu_k}{K}\right)^2 + \left(\frac{\mu_m}{K}\right)^2} \times \left[\frac{\nu_k}{k}\cosh\frac{\nu_k}{k}\ell_2 \sin\frac{\mu_m}{k}\ell_2 - \frac{\mu_m}{k}\sinh\frac{\nu_k}{k}\ell_2\cos\frac{\mu_m}{k}\ell_2\right] \tag{A1}$$

$$G_2(\nu,\mu) = \frac{1}{\left(\frac{\nu_k}{K}\right)^2 + \left(\frac{\mu_m}{K}\right)^2} \times \left[\frac{\nu_k}{K}\sinh\frac{\nu_k}{K}\ell_2 \cos\frac{\mu_m}{K}\ell_2 - \frac{\mu_m}{K}\cosh\frac{\nu_k}{K}\ell_2\sin\frac{\mu_m}{K}\ell_2\right] \tag{A2}$$

$$g_1(\nu) = a_4\frac{\nu_k}{K}\cosh\frac{\nu_k\ell_2}{K} + b_4\sinh\frac{\nu_k\ell_2}{K} \tag{A3}$$

$$g_2(\nu) = a_4\frac{\nu_k}{K}\sinh\frac{\nu_k\ell_2}{K} + b_4\cosh\frac{\nu_k\ell_2}{K} \tag{A4}$$

$$\left(\frac{\mu}{K}\ell_2\right)\cot\left(\frac{\mu}{K}\ell_2\right) + \frac{b_4}{a_4}\ell_2 = 0 \tag{A5}$$

$$\left(\frac{\mu}{K}\ell_2\right)\tan\left(\frac{\mu}{K}\ell_2\right) = \frac{b_4}{a_4}\ell_2 \tag{A6}$$

Thus, for $t \to \infty$, the present work is reduced to the steady-state thermal behavior analysis of Aköz and Tauchert; also Table 1 of this limiting case then reduces to the corresponding table in Ref. 16.

References

[1]Poon, K. C. and Chang, Y. P., "Transformation of Heat Conduction Problems from Anisotropic to Isotropic," *Letters in Heat and Mass Transfer*, Vol. 5, 1978, p. 215.

[2]Chu, H. S., Weng, C. I., and Chen, C. K., "Transient Response of a Composite Straight Fin," *ASME Journal of Heat Transfer*, Vol. 105, 1983, pp. 307-311.

[3]Chang, Y. P., "Analytical Solution for Heat Conduction in Anisotropic Media in Infinite, Semi-Infinite and Two-Plane-Bounded Regions," *International Journal of Heat and Mass Transfer*, Vol. 20, 1977, p. 1019.

[4]Huang, S. C. and Chang, Y. P., "Heat Conduction in Unsteady, Periodic, and Steady States in Laminated Composites," *ASME Journal of Heat Transfer*, Vol. 102, 1980, pp. 742-748.

[5]Tauchert, T. R. and Aköz, A. Y., "Stationary Temperature and Stress Fields in Anisotropic Elastic Slab," *ASME Journal of Applied Mechanics*, Vol. 42, 1974, pp. 647-650.

[6]Katayama, K., Saito, A., and Kobayashi, N., "Transient Heat Conduction in Anisotropic Solids," *Proceedings of the International Conference on Heat and Mass Transfer*, Tokyo, 1974, p. 137.

[7]Sharma, B., "Thermal Stresses in Transversely Isotropic Semi-Infinite Elastic Solid," *Journal of Applied Mechanics*, Vol. 25, 1958, pp. 86-88.

[8]Mossakoska, Z. and Nowacki, W., "Thermal Stresses in Transversely Isotropic Bodies," *Archiv Mech. Stosow.*, Vol. 10, No. 4, 1958, pp. 569-603.

[9]Singh, A., "Axisymmetric Thermal Stresses in Transversely Isotropic Bodies," *Archiv Mech. Stosow.*, Vol. 39, No. 3, 1960, pp. 287-304.

[10]Sugano, Y., "Transient Thermal Stresses in a Transversely Isotropic Finite Circular Cylinder Due to an Arbitrary Internal Heat-Generation," *International Journal of Engineering Science*, Vol. 17, 1979, pp. 729-939.

[11]Sugano, Y. and Takeuti, Y., "Transient Thermal Stresses in a Transversely Isotropic Thick Plate with a Cylindrical Hole Due to Surface Heat-Generation," *Proceedings of the 5th International Conference on SMIRT*, Vol. M-11/4, 1980, pp. 159-183.

[12]Takeuti, Y. and Noda, N., "A General Treatise on the Three-Dimensional Thermoelasticity of Curvilinear Aeolotropic Solids," *Journal of Thermal Stresses*, Vol. 1, 1978, pp. 25-39.

[13]Noda, N., "Transient Thermal Stress Problem in a Transversely Isotropic Finite Circular Cylinder Under Three-Dimensional Temperature Field," *Journal of Thermal Stresses*, Vol. 6, 1983, pp. 57-71.

[14]Aköz, A. Y. and Tauchert, T. R., "Thermal Stresses in an Orthotropic Elastic Semispace," *Journal of Applied Mechanics*, Vol. 39, 1972, pp. 87-90.

[15]Tauchert, T. R. and Aköz, A. Y., "Thermal Stresses in an Orthotropic Elastic Slab Due to Prescribed Surface Temperatures," *Journal of Applied Mechanics*, Vol. 41, 1974, pp. 222-228.

[16]Aköz, A. Y. and Tauchert, T. R., "Thermoelastic Analysis of a Finite Orthotropic Slab," *Journal of Mechanical Engineering Science*, Vol. 20, 1978, pp. 65-71.

[17]Wang, H. S. and Chou, T. W., "Transient Thermal Stress Analysis of a Rectangular Orthotropic Slab," submitted for publication.

[18]Carslaw, H. S. and Jaeger, J. C., *Conduction of Heat in Solids*, Clarendon Press, Oxford, England, 1959.